DE GRUYTER OPEN Open Geosci. 2015; 7:223–233

Research Article Open Access

Hilary Downes*, Andrew Carter, Richard Armstrong, Gabor Dobosi, and Antal Embey-Isztin

Lower crustal zircons reveal Neogene metamorphism beneath the Pannonian Basin (Hungary)

DOI 10.1515/geo-2015-0028

Received August 25, 2014; accepted January 27, 2015

Abstract: Neogene alkaline intraplate volcanic deposits in the Pannonian Basin (Hungary) contain many lower crustal granulite-facies xenoliths. U-Pb ages have been determined for zircons separated from a metasedimentary xenolith, using LA-ICPMS and SHRIMP techniques. The zircons show typical metamorphic characteristics and are not related to the host magmatism. The oldest age recorded is late Devonian, probably related to Variscan basement lithologies. Several grains yield Mesozoic dates for their cores, which may correspond to periods of orogenic activity. Most of the zircons show young ages, with some being Palaeocene-Eocene, but the majority being younger than 30Ma. The youngest zircons are Pliocene (5.1-4.2 Ma) and coincide with the age of eruptions of the host alkali basalts. Such young zircons, so close to the eruption age, are unusual in lower crustal xenoliths, and imply that the heat flow in the base of the Pannonian Basin was sufficiently high to keep many of them close to their blocking temperature. This suggests that metamorphism is continuing in the lower crust of the region at the present day.

Keywords: xenolith; zircons; lower crust; Pannonian Basin

***Corresponding Author: Hilary Downes:** Department of Earth and Planetary Sciences, Birkbeck University of London, Malet Street, London WC1E 7HX, UK., E-mail: h.downes@ucl.ac.uk
Andrew Carter: Department of Earth and Planetary Sciences, Birkbeck University of London, Malet Street, London WC1E 7HX, UK
Richard Armstrong: Research School of Earth Sciences, The Australian National University Canberra 0200 A.C.T. Australia
Gabor Dobosi: Research School of Earth Sciences, The Australian National University Canberra 0200 A.C.T. Australia
Gabor Dobosi: MTA MTA-ELTE Volcanology Research Group, H-1117 Budapest, Pázmány Péter sétány 1/C, Hungary
Antal Embey-Isztin: Department of Mineralogy and Petrology, Hungarian Natural History Museum, Ludovika tér 2, H-1083 Budapest, Hungary

1 Introduction

Zircons from within granulite xenoliths can be used to date events within the lower crust [1]. Lower crustal zircon ages often show a correspondence with overlying crustal ages, e.g. the oldest zircon ages are 2.5-3.5 Ga in granulite xenoliths from beneath the Archaean Fennoscandian shield [2, 3], and those in granulite xenoliths from the Siberian craton yield ages of 1.8-1.9 Ga consistent with the ages of metamorphism in the region [4]. Younger lower crustal zircon ages showing a peak at 280 Ma are found in granulite xenoliths from beneath the late- Palaeozoic Variscan orogenic belt of western Europe [5], but nevertheless they are still far older than the age of the Neogene eruption that brought them to the surface. Here we present new U- Pb determinations on zircons separated from a lower crustal metasedimentary granulitic xenolith from the Pannonian Basin of Hungary, and demonstrate that some yield extremely young dates (ca.4-9 Ma), indicating that the lower crust was still experiencing high temperature metamorphism when the xenolith was entrained in the Neogene host alkali basalt magma.

2 Geological background

The Pannonian Basin (Figure 1) is an extensional back-arc basin within the Alpine-Carpathian-Dinaride orogenic belt of central-eastern Europe [6]. Plate tectonic reconstructions [7] show a complex interplay of microcontinents and oceans during the late Mesozoic, followed by final docking in the Cenozoic. Rapid tectonic collapse and basin formation occurred in Neogene times and was controlled by a combination of gravitational collapse of a former overthickened orogenic belt [8], subduction roll-back along the Carpathian arc [9] and asthenosphere updoming. The area is characterized by thin crust, 25-30 km thick [10, 11] and thinned lithosphere (Figure 1) with the base of the lithosphere at a depth of only ca. 60 km [10]. The Pannonian

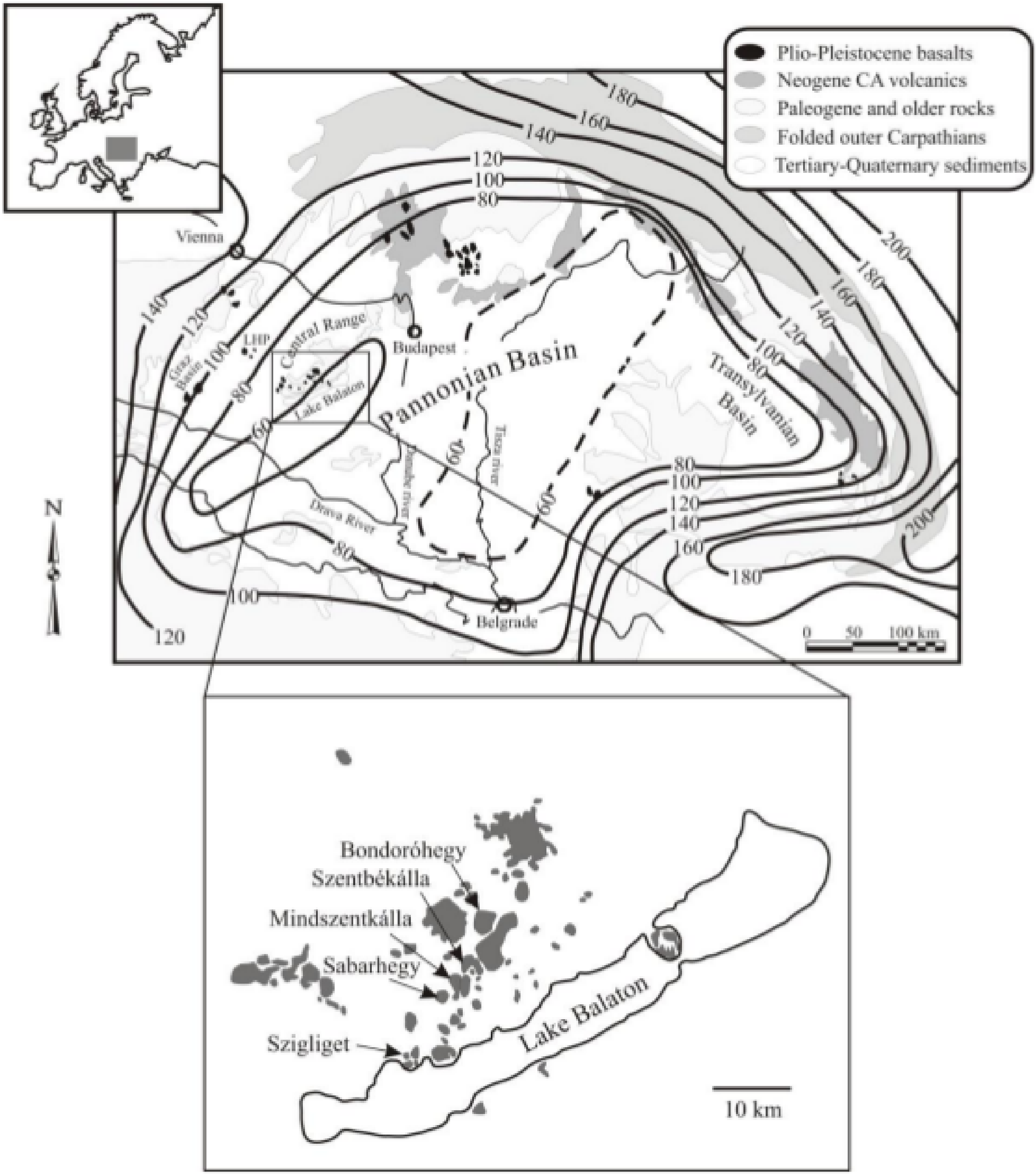

Figure 1: Sketch map of the Pannonian Basin (inset shows geographical location), with contours of the base of the lithosphere. The area shown in the lower figure is the Neogene volcanic region of the Balaton Highlands, indicating where the sample was collected.

Basin is a region of very high heat-flow with a mean value of 100 mW/m^2 [12] and Moho temperatures of ca. 900°C [13]. Hence the present-day conditions within the lower crust of this region are appropriate for high-temperature, low-pressure metamorphism.

Neogene intraplate alkaline volcanism in the Pannonian Basin has entrained numerous xenoliths of mantle and lower crustal origin [14, 15]. The sample analysed in this study was found in basaltic tuffs near the village of Mindszentkalla (Figure 1) in the Balaton Highlands [16]. Although the absolute age of the host pyroclastic deposit has not been determined, many nearby phreatomagmatic eruptions occurred during a volcanic phase from 4.2 to 4.8 Ma [17], so the host tuff is probably of similar age.

The petrology and geochemistry of lower crustal granulite xenoliths from the Pannonian Basin have been previous studied [15, 16, 18–22]. Most of the xenoliths are garnetiferous mafic meta-igneous rocks, but in contrast to the lower continental crust worldwide, they show some unusual chemical features such as LREE-depletion and positive ϵNd isotope compositions that have been interpreted as indicating that their protolith was of MORB composition. This suggests that they originated as ocean crust that accreted to the lithosphere during subduction [19]. The garnet-rich nature of the granulite suite is surprising, given the present-day thin crust. Pressure estimates for the xenoliths are 8-15 kbar [16, 23], which suggests a crustal thickness of 40-50 km instead of the present-day value of <30 km. Thus their pressure estimates refer to conditions that existed prior to the Neogene tectonic collapse of the Pannonian Basin.

The studied sample M3044 is a relatively fresh metasedimentary garnet granulite xenolith, consisting largely of plagioclase (48%), garnet (34%) and biotite (15%), with 2-3% graphite, zircon and traces of spinel (Figure 2). Its associated mafic granulite xenoliths yield temperatures of 800-950°C [16]. Similar high temperatures (850-1050°C) in lower crustal xenoliths from the same region have been inferred by [22].

The xenolith location is situated on the Alcapa terrane [7], part of the Apulian indenter that moved northwards during Cretaceous-Palaeogene continental collision and was locked into its present-day position in Late Miocene times [24]. Although rocks of Ordovician and Silurian age occur in the upper crust of this unit, the main crystalline upper crustal lithologies are Variscan granites, gneisses and amphibolites [25]. Many of these lithologies are also present as xenoliths, together with Permian sandstones, and Mesozoic and Cenozoic sedimentary rocks.

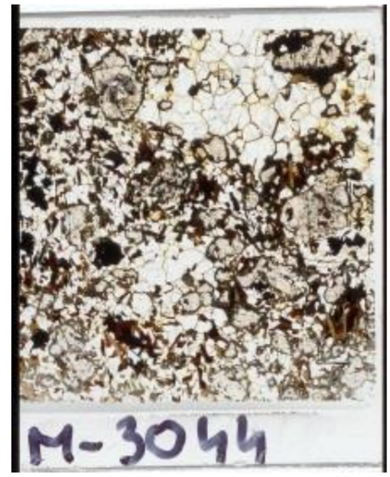

Figure 2: Thin-section photomicrograph of sample M3044 in plane polarized light. Field of view 26 mm.

3 Geochronology methods

Small interior pieces of sample M3044 were crushed in a shatter box and then sieved through a disposable cloth; the heavy mineral fractions were extracted using heavy liquids. Particular care was taken to avoid contamination at all stages. Zircons were hand-picked from the concentrate and mounted in epoxy. The analysed zircons tend to be rounded; they range in size from 100 to 250 μm. Cathodoluminescence (CL) images show complex zoning (Figure 3); some zircons have dark rounded cores and lighter rims. SHRIMP UPb analyses were made of areas that appeared homogeneous in CL, whereas the LA-ICPMS analyses took no account of zoning.

An initial survey of 49 zircons was undertaken for U-Pb dating by LA-ICPMS at UCL/Birkbeck using a New Wave 213 aperture imaged frequency quintupled laser ablation system (213 nm) coupled to an Agilent 750 quadrupole-based ICP–MS. The laser spot size was 50 μm. Real-time data were processed using GLITTER. Repeated measurements of external zircon standard PLESOVIC (TIMS reference age 337.1±0.7 Ma [26]) and NIST 612 silicate glass [27] were used to correct for instrumental mass bias and depth-dependent inter-element fractionation of Pb, Th and U. Data were filtered using standard discordance tests with a 10% cutoff and common Pb was determined by the ^{208}Pb method assuming a common Pb composition from the age-dependent Pb model of [28]. Data were processed using Isoplot [29]. Results are given in Table 1 and shown on a concordia diagram in Figure 4.

Additional U-Pb analyses of 9 zircons were subsequently made using the SHRIMP II at the Research School

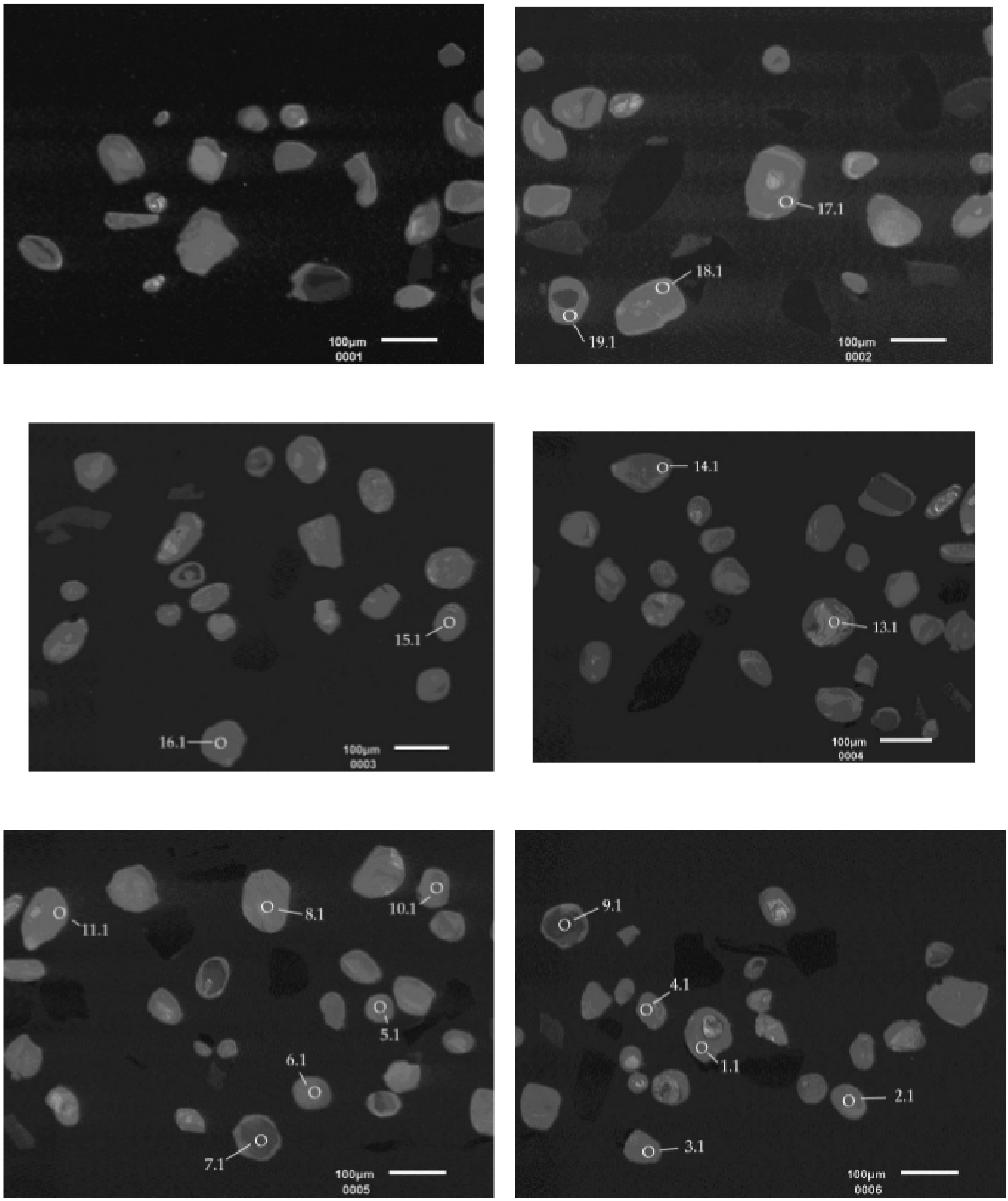

Figure 3: CL images of zircons separated from metasedimentary granulite xenolith M3044 highlighting those analysed by SHRIMP (Table 1).

Table 1: LA-ICPMS data for zircons from M3044.

Grain	U ppm	Th /U	Uncorrected ratios $^{206}Pb/^{238}U$	1 se %	$^{207}Pb/^{235}U$	1se %	$^{207}Pb/^{206}Pb$	1se %	% Com Pb	Uncorrected ages (Myr) $^{206}Pb/^{238}U$	2 σ	$^{207}Pb/^{235}U$	2 σ	$^{207}Pb/^{206}Pb$	2 σ	% discord	^{208}Pb corrected ages (Myr) $^{206}Pb/^{238}U$	2 σ	$^{207}Pb/^{235}U$	2 σ	$^{207}Pb/^{206}Pb$	2 σ	% discord
HD1	48	0.37	0.00268	3.0	0.01957	20.4	0.05808	20.5	0.92	17.3	1.2	19.7	8.1	532.8	449.8	12.3	17.4	0.9	18.7	2.7	229.8	191.0	6.9
HD2	119	0.17	0.01422	1.1	0.09196	3.8	0.05189	3.8	0.06	91.0	2.1	89.3	7.1	280.6	86.0	-1.9	92.4	1.2	97.4	53.8	257.5	1241.2	5.1
HD3	108	0.22	0.00108	3.7	0.00937	19.6	0.06971	19.9	0.89	7.0	0.9	9.5	3.8	919.8	408.8	26.5	6.9	0.7	9.4	3.3	698.8	716.0	26.5
HD4	131	0.65	0.00102	2.9	0.01023	12.5	0.08162	12.8	-5.11	6.6	0.8	10.3	2.7	1236.4	250.8	36.4	9.0	0.7	18.1	7.6	1975.0	53.5	50.0
HD5	120	0.23	0.02228	0.9	0.15357	2.6	0.05533	2.5	0.21	142.0	2.8	145.1	8.2	425.6	56.8	2.1	144.4	1.5	154.5	12.6	354.2	170.7	6.5
HD6	143	0.23	0.0096	1.0	0.06225	3.7	0.05317	3.7	0.16	61.6	1.5	61.3	4.7	336.1	84.0	-0.4	62.7	1.0	67.4	27.7	280.9	923.1	6.9
HD7	134	0.30	0.00096	2.1	0.00924	13.2	0.07807	13.4	2.38	6.2	0.7	9.3	2.6	1148.7	265.6	33.8	5.8	0.7	7.8	1.8	585.7	362.0	25.0
HD8	104	0.05	0.00358	1.7	0.02456	8.7	0.0551	8.7	0.71	23.0	1.0	24.6	4.4	416.3	195.0	6.5	22.6	0.8	24.3	3.1	167.6	86.3	7.1
HD9	457	0.05	0.02478	0.8	0.17236	1.8	0.05079	1.8	0.19	157.8	2.8	161.5	6.2	231.3	40.9	2.3	157.5	1.5	157.6	34.8	158.7	485.9	0.1
HD10	359	0.07	0.00105	1.9	0.00643	11.2	0.04489	11.4	-0.01	6.8	0.7	6.5	1.6	-61.6	277.1	-4.0	6.8	0.7	6.6	2.8	-59.0	984.3	-3.5
HD11	157	0.17	0.00107	1.9	0.01137	10.4	0.08583	10.6	2.71	6.9	0.7	11.5	2.5	1334.4	204.4	39.9	6.3	0.7	9.4	3.0	772.4	126.8	32.8
HD12	110	0.23	0.01496	1.1	0.09664	3.6	0.05264	3.6	0.40	95.7	2.2	93.7	7.1	313.3	80.8	-2.2	96.6	1.3	98.1	7.6	165.1	156.5	1.5
HD13	130	0.15	0.02295	1.0	0.16113	2.9	0.05711	2.8	-0.37	146.3	3.0	151.7	9.4	495.8	61.0	3.6	150.5	1.6	177.3	20.6	605.9	230.7	15.1
HD14	113	0.04	0.00789	1.5	0.04941	6.7	0.04813	6.6	0.24	50.7	1.7	49.0	6.7	105.7	157.1	-3.5	50.4	1.0	49.7	12.1	7.9	574.8	-1.5
HD15	210	0.20	0.00132	1.5	0.00922	9.5	0.0572	9.6	1.27	8.5	0.7	9.3	1.9	499.3	211.8	8.7	8.3	0.7	8.6	2.3	52.2	409.4	3.2
HD16	77	0.23	0.00972	1.3	0.12446	3.9	0.10342	3.8	3.67	62.4	1.8	119.1	9.9	1686.4	70.7	47.6	55.5	1.1	94.7	6.7	1085.2	61.9	41.4
HD17	356	0.07	0.0322	0.9	0.23795	2.0	0.05374	1.9	-0.33	204.3	3.8	216.7	9.6	360.2	42.4	5.7	207.9	2.0	227.5	52.7	467.9	469.1	8.6
HD18	115	0.12	0.00266	1.9	0.01874	10.5	0.05684	10.5	1.96	17.1	0.9	18.9	4.0	485.3	232.7	9.2	16.2	0.8	14.9	2.6	-279.9	189.4	-8.4
HD19	157	0.21	0.0204	1.0	0.14839	2.7	0.0581	2.5	0.47	130.2	2.7	140.5	8.1	533.5	55.4	7.3	130.8	1.5	143.8	9.5	384.6	126.1	9.0
HD20	123	0.13	0.02641	1.0	0.18456	2.8	0.05498	2.6	-0.55	168.0	3.4	172.0	10.6	411.4	59.0	2.3	173.5	1.8	200.0	18.5	584.1	182.6	13.2
HD21	475	0.07	0.00735	1.2	0.05925	4.3	0.05912	4.2	0.36	47.2	1.3	58.4	5.2	571.5	92.0	19.2	47.0	0.9	56.1	5.1	462.0	184.4	16.3
HD22	128	0.23	0.00923	1.2	0.06496	4.2	0.05633	4.1	0.33	59.2	1.6	63.9	5.6	465.4	91.2	7.3	60.0	1.0	66.9	16.2	359.1	530.4	10.3
HD23	117	0.06	0.00326	2.1	0.02267	11.2	0.05562	11.3	1.91	21.0	1.1	22.8	5.2	437.2	250.9	7.8	19.7	0.8	17.9	2.2	-333.7	248.1	-10.3
HD24	358	0.13	0.00932	1.1	0.09079	2.9	0.06982	2.7	-1.18	59.8	1.5	88.2	5.4	923.1	55.9	32.2	63.2	0.9	99.5	11.8	1176.6	222.1	36.5
HD25	172	0.08	0.00427	1.6	0.03526	7.0	0.06456	7.0	0.60	27.5	1.1	35.2	5.0	760.0	146.7	21.9	27.1	0.8	34.9	3.9	596.7	121.9	22.4
HD26	163	0.28	0.01909	1.0	0.13169	3.3	0.05504	3.0	2.60	121.9	2.7	125.6	8.7	413.8	66.6	3.0	113.6	1.5	84.9	15.0	-790.8	480.8	-33.8
HD27	129	0.18	0.00784	1.3	0.05545	5.0	0.05686	4.8	1.44	50.3	1.5	54.8	5.6	486.1	106.0	8.1	48.6	1.0	47.9	5.5	-39.6	180.9	-1.5
HD28	112	0.22	0.03113	1.1	0.20328	3.4	0.05316	3.0	-0.68	197.6	4.3	187.9	14.0	335.6	68.6	-5.2	207.1	2.2	229.6	99.9	556.0	888.8	9.8
HD29	150	0.19	0.00083	3.6	0.00635	19.8	0.06004	20.0	1.89	5.3	0.8	6.4	2.6	605.0	433.4	16.8	5.1	0.7	5.1	2.2	-56.2	972.2	0.5
HD30	400	0.66	0.00086	2.3	0.01467	7.0	0.12302	7.1	7.11	5.5	0.7	14.8	2.2	2000.5	126.8	62.5	4.2	0.7	7.9	4.4	951.6	175.5	47.5
HD31	174	0.19	0.01862	1.2	0.12079	4.5	0.05116	4.1	-0.35	118.9	3.0	115.8	10.9	248.0	93.6	-2.7	122.7	1.7	132.4	16.0	372.6	255.1	7.3
HD32	130	0.10	0.00671	1.3	0.04902	5.5	0.05807	5.2	0.17	43.1	1.3	48.6	5.5	532.4	114.6	11.3	43.3	0.9	51.8	17.1	480.4	715.0	16.5
HD33	181	0.53	0.00097	2.1	0.01094	10.3	0.08801	10.4	1.65	6.2	0.7	11.0	2.4	1382.7	199.7	43.4	6.2	0.7	10.0	2.7	1076.9	310.1	37.7
HD34	77	0.06	0.00469	2.1	0.0319	10.4	0.05395	10.3	1.25	30.2	1.5	31.9	6.7	369.0	231.3	5.4	29.0	0.9	28.1	18.0	-114.8	1567.6	-3.3
HD36	252	0.65	0.00091	3.3	0.01445	10.8	0.12541	11.0	4.80	5.9	0.8	14.6	3.2	2034.6	194.6	59.7	5.0	0.7	10.9	12.3	1431.9	115.9	53.9
HD35	213	0.65	0.04327	1.2	0.30163	4.0	0.05629	3.3	-4.49	273.1	6.5	267.7	24.0	463.8	73.6	-2.0	363.5	3.5	466.2	59.2	1493.8	194.9	22.0
HD37	113	0.10	0.00424	1.9	0.0322	8.0	0.06094	7.8	1.15	27.3	1.2	32.2	5.2	637.1	167.0	15.2	26.4	0.9	29.9	8.6	276.0	646.4	11.8
HD38	93	0.08	0.00332	2.4	0.02234	13.2	0.05485	13.2	1.16	21.4	1.2	22.4	6.0	406.1	294.6	4.8	20.7	0.9	20.7	3.0	-26.9	299.3	0.3
HD39	161	0.25	0.00749	1.5	0.04899	5.8	0.05151	5.4	-0.38	48.1	1.6	48.6	5.8	263.7	123.4	0.9	50.1	1.0	55.9	8.2	396.0	152.5	10.4
HD40	168	0.25	0.03965	1.2	0.25587	4.1	0.05168	3.4	1.27	250.7	6.1	231.3	21.1	271.3	77.6	-8.4	244.9	3.1	204.3	154.7	-270.4	1876.3	-19.9
HD41	163	0.44	0.00139	2.9	0.03463	7.4	0.20208	7.4	14.79	9.0	0.9	34.6	5.2	2843.1	121.2	74.1	4.4	0.7	17.7	3.7	1717.4	368.3	75.1

Table 1: Continued.

Grain	U ppm	Th /U	$^{206}Pb/^{238}U$	1 se %	$^{207}Pb/^{235}U$	1se %	$^{207}Pb/^{206}Pb$	1se %	% Com Pb	Uncorrected ages (Myr) $^{206}Pb/^{238}U$	2 σ	$^{207}Pb/^{235}U$	2 σ	$^{207}Pb/^{206}Pb$	2 σ	% discord	^{208}Pb corrected ages (Myr) $^{206}Pb/^{238}U$	2 σ	$^{207}Pb/^{235}U$	2 σ	$^{207}Pb/^{206}Pb$	2 σ	% discord
HD42	194	0.20	0.00107	2.8	0.00607	19.8	0.04591	19.8	1.04	6.9	0.8	6.1	2.5	-7.1	477.4	-12.2	6.8	0.7	5.5	4.2	-523.1	238.5	-21.9
HD43	1967	0.02	0.03325	1.2	0.22246	4.1	0.04815	3.3	0.02	210.9	5.2	204.0	18.2	106.6	77.0	-3.4	211.1	2.6	201.8	103.2	97.3	1151.4	-4.6
HD44	218	0.30	0.00077	2.6	0.00661	16.9	0.06858	17.0	2.50	5.0	0.7	6.7	2.4	886.1	351.4	25.8	4.6	0.7	5.1	1.5	141.8	223.0	9.9
HD45	564	0.11	0.00652	1.4	0.04282	5.1	0.04752	4.5	- 0.34	41.9	1.3	42.6	4.5	75.4	106.0	1.6	42.8	0.9	45.0	17.9	207.9	909.0	4.9
HD46	194	0.31	0.00118	2.5	0.01076	13.5	0.07393	13.4	3.28	7.6	0.8	10.9	3.0	1039.6	269.8	30.0	6.9	0.7	7.7	1.8	112.2	391.9	10.2
HD47	212	0.06	0.00459	1.7	0.03503	6.7	0.06095	6.2	0.91	29.5	1.2	35.0	4.8	637.5	133.8	15.6	28.7	0.9	33.6	15.3	356.5	1020.2	14.5
HD48	225	0.16	0.00089	4.5	0.00487	26.5	0.04516	26.6	0.11	5.7	0.9	4.9	2.7	-47.0	646.8	-16.3	5.8	0.7	5.5	3.0	-93.6	1300.5	-5.6
HD49	220	0.20	0.00073	4.1	0.00388	26.8	0.0438	26.8	0.72	4.7	0.8	3.9	2.2	-121.9	660.3	-19.6	4.7	0.7	3.8	1.3	-488.1	670.9	-21.8
HD50	195	0.27	0.00294	2.0	0.01925	9.2	0.05357	8.8	- 0.92	18.9	1.0	19.4	3.7	353.0	199.5	2.3	20.2	0.8	25.0	0.9	636.9	52.9	19.4

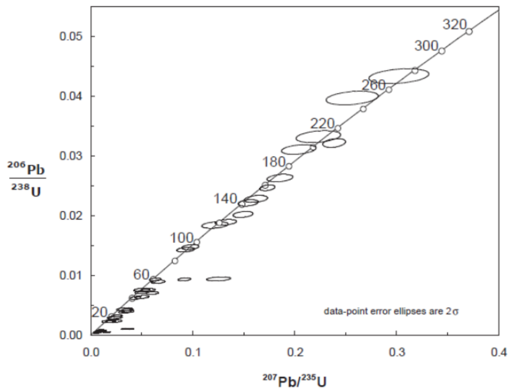

Figure 4: Concordia plot for U-Pb data from zircons from xenolith M3044 by LA-ICPMS (data from Table 1).

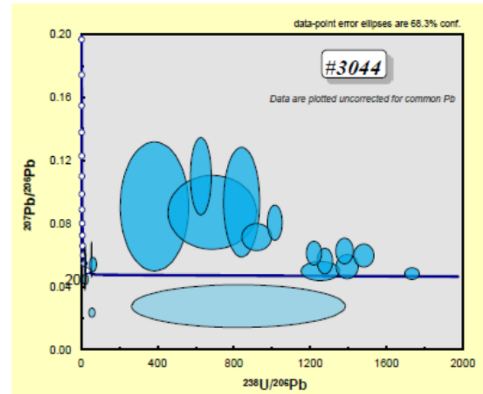

Figure 5: Tera-Wasserburg diagram for zircons from xenolith M3044 analysed by SHRIMP (data from Table 2).

of Earth Sciences, The Australian National University, using the standard analytical protocols described by [30]. A mass-filtered primary O2-beam was focused onto the zircons producing a spot size of approximately 20μm in diameter. The surface was rastered for 2.5 minutes before analysis. Data acquisition was done by repeatedly stepping through the masses $^{90}Zr_{2}^{1}6O$ ("reference mass 196"), ^{204}Pb, background at mass 204.04, ^{206}Pb, ^{207}Pb, ^{208}Pb, ^{238}U, ^{232}Th and $^{238}U^{16}O$ (mass 254), for 6 scans.

The data were reduced in a manner similar to that described by [30], using the SQUID I Excel Macro [31]. The reference zircon Temora II (416.8 ± 1.3 Ma [32]) was the primary U-Pb calibration standard, with standard zircon SL13 (U concentration of 238 ppm [33]) used to calibrate the U, Pb and Th concentrations. Decay constants given in [34] were used in the age calculations. Uncertainties given for individual U-Pb analyses (ratios and ages) are at the 1σ level, however uncertainties in the calculated weighted mean ages are reported as 95% confidence limits and include the uncertainties in the standard calibrations where appropriate. For the age calculations, corrections for common Pb were made using the measured ^{204}Pb and the relevant common Pb compositions from the [35] model. Concordia plots, regressions and any weighted mean age calculations were carried out using Isoplot/Ex 3.0 [29] and where relevant include the error in the standard calibration. SHRIMP results are presented in Table 2 and plotted on Tera-Wasserburg type concordia plot uncorrected for common Pb (Figure 5).

4 Results

Zircons analysed by LA-ICPMS show a wide range of ages from 4.2 Ma to 363 Ma (Table 1), although most are Cenozoic. Their ages are mostly concordant (Figure 4), although some younger zircons (<60 Ma) are discordant. A relative probability plot of the LA-ICPMS results is shown in Figure 6. Over half of the analysed zircon grains (26 out of 49) yielded ages younger than 30 Ma, with the youngest dates being Pliocene (4.2 - 5.1 Ma). Ten further grains yielded a variety of Palaeocene or Eocene ages (63.2-42.8 Ma). Nine grains are Jurassic and Cretaceous (173-92 Ma) and two grains have identical late Triassic ages (207 Ma). One zircon yielded an early Triassic date (245 Ma) and the oldest grain is Late Devonian (363 Ma).

In general, the age data obtained from the SHRIMP analysis agree with those obtained by LA-ICPMS, even though the volume of zircon analysed by the two methods differs greatly. One zircon (spot 16.1) yielded a late Devonian age (372.8 ± 38 Ma), similar to the oldest date determined by LA-ICPMS. Three zircons yielded Jurassic-Cretaceous dates (125-106 Ma), and the remaining zircons gave young dates from 15.9 ± 5 Ma to 3.7 ± 0.1 Ma. Clearly the analyses are scattered and some also have high uncertainties. The reasons for this are (a) these zircons are young and have low radiogenic Pb contents and (b) they show complex micro-zoning of Pb isotopes which deserves further investigation in future studies.

5 Discussion

Zircons from M3044 are generally rounded, typical of metamorphic zircons [36]. Igneous zoning was not observed, and the zircons are clearly not related to the host alkali basaltic magmatism. Given the high equilibration temperature of the Hungarian xenoliths (800-950°C) and the high Moho temperature (900°C), we suggest that metamorphism was still on-going at the time when the xeno-

Table 2: Summary of SHRIMP U-Pb zircon data for sample 3044.

Grain. Spot	% ^{206}Pb	ppm U	ppm Th	^{232}Th $/^{238}U$	ppm ^{206}Pb	Total ^{238}U $/^{206}Pb$	±%	Total ^{207}Pb $/^{206}Pb$	±%	(2) ^{206}Pb $/^{238}U$	±%	^{206}Pb $/^{238}U$ Age	±%
1.1	5.99	108	16	0.16	0.1	840.44	7.4	0.0935	24.3	0.00112	0.00009	7.2	0.6
2.1	5.19	165	24	0.15	0.2	684.28	22.3	0.0872	17.6	0.00139	0.00031	8.9	2
3.1	2.1	368	137	0.38	0.2	1381.56	2.2	0.0627	8.5	0.00071	0.00002	4.6	0.1
4.1	0.52	378	94	0.26	0.3	1253.69	5.3	0.0502	8	0.00079	0.00004	5.1	0.3
5.1	-2.31	350	151	0.45	0.4	824.12	45	0.028	31.8	0.00124	0.00056	8	3.6
6.1	5.63	174	13	0.08	0.4	381.94	31.1	0.0908	29.3	0.00247	0.00077	15.9	5
7.1	0.33	1418	112	0.08	0.7	1735.43	1.4	0.0487	4.9	0.00057	0.00001	3.7	0.1
8.1	8.08	86	13	0.16	0.1	625.73	5.9	0.11	14.6	0.00147	0.00009	9.5	0.6
9.1	1.12	2077	239	0.12	35.3	50.61	1	0.0575	12.9	0.01954	0.00028	124.7	1.7
10.1	4.37	184	58	0.33	0.2	1014.26	2.4	0.0807	9.1	0.00094	0.00002	6.1	0.2
11.1	1.93	350	137	0.41	0.2	1220.04	2.1	0.0614	8.1	0.0008	0.00002	5.2	0.1
12.1	1.29	291	127	0.45	0.2	1277.87	2.1	0.0563	9.5	0.00077	0.00002	5	0.1
13.1	-0.01	773	354	0.47	12.8	51.81	1.1	0.0484	1.5	0.0193	0.00022	123.2	1.4
14.1	1.73	446	197	0.46	0.3	1482.89	2.4	0.0598	7.9	0.00066	0.00002	4.3	0.1
15.1	-3.06	74	6	0.09	1.2	52.62	22.2	0.0242	7.7	0.01959	0.00436	125	27.6
16.1	-0.28	278	56	0.21	14.2	16.85	10.3	0.0518	17.1	0.05953	0.00626	372.8	38.1
17.1	3.24	220	48	0.22	0.2	918.51	5.5	0.0717	7.8	0.00105	0.00006	6.8	0.4
18.1	0.88	368	144	0.41	0.2	1395.3	2.8	0.053	9.4	0.00071	0.00002	4.6	0.1
19.1	0.8	127	8	0.07	1.8	59.83	19.7	0.0545	5.3	0.01658	0.00328	106	20.8

Errors are 1-sigma; Pb_c and Pb* indicate the common and radiogenic portions, respectively.
Error in Standard calibration was 0.21% (not included in above errors but required when comparing data from different mounts).
(2) Common Pb corrected by assuming $^{206}Pb/^{238}U$-$^{207}Pb/^{235}U$ age-concordance.

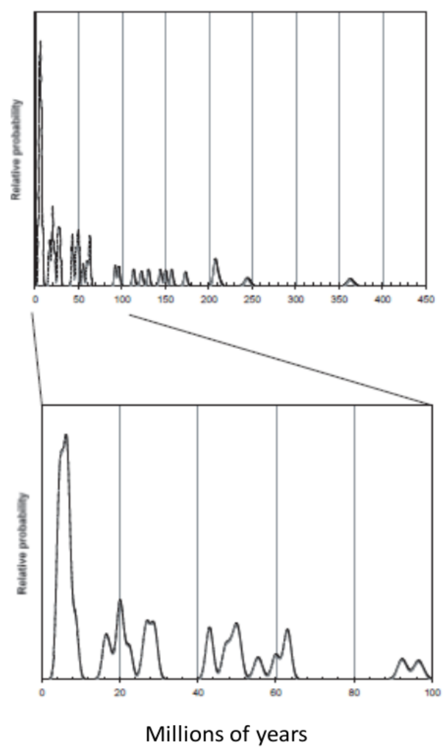

Figure 6: Relative probability plot of ages for zircons from xenolith M3044 by LA-ICPMS (data from Table 1).

liths were exhumed. The only other region of Europe in which lower crustal xenoliths yield such high temperatures (900°C) is the Neogene volcanic zone of SE Spain [37].

The oldest dates (Late Devonian) recorded in the zircons must be inherited and are probably derived from the Palaeozoic crystalline basement lithologies. The late Mesozoic (90-100 Ma) and Palaeogene ages (40-65 Ma) may be associated with Alpine orogenic cycles and collision [7]. The large group of dates between 32 and 15 Ma may relate to tectonic episodes within the Pannonian Basin. The younger ages (15-16 Ma) coincide with the first phase of extension in the Pannonian Basin. However, the most abundant zircon ages are Mio-Pliocene (Figure 6). The youngest dates must be close to the age of eruption of the host basaltic tuff. This is confirmed by the youngest SHRIMP age of 3.7 ± 0.1 Ma.

It is rare for zircons in granulite xenoliths to record an age so close to that of their magmatic host. Granulite xenoliths in Cenozoic basalts from China yield ages as young as 90 Ma, recording the peak of zircon growth related to asthenospheric uprise beneath eastern China [38]. Metasedimentary granulite xenoliths from the Variscan belt of central France [5] show a wide variation in zircon ages (630-150 Ma) but nevertheless the youngest dates are more than 140 Ma older than the age of the host eruption. Zircons in a felsic granulite xenolith from central Spain [39] range from 590 to 250 Ma, the latter age being coeval with the magmatic host and recorded only in rims. However, no metamorphic zircons as young as 3.7 Ma have previously been recorded from the continental lower crust. This suggests that many of the zircon crystals in M3044 were still above their blocking temperature when the xenolith was entrained in the host eruption. Although it has been suggested that zircon ages may post-date peak metamorphic conditions [40], nevertheless the young ages seen in zircons from M3044 imply that the lower crust was experiencing very high temperature conditions in late-Miocene times. These metamorphic conditions were probably a result of the Neogene tectonic collapse of the region, crustal thinning, and asthenospheric upwelling.

6 Conclusions

Zircons separated from a metasedimentary lower crustal granulite xenolith from the Pannonian Basin region (Hungary) yield young ages (4-9 Ma), the youngest of which are coeval with the probable eruption age of the magmatic host. The ages are interpreted as indicating that high temperature metamorphism was continuing in the lower crust of the region at the time of entrainment of the xenolith, such that the zircons were above their blocking temperature. This is in agreement with the geological setting of the Pannonian Basin, which is a region of recently- thinned continental lithosphere and high heat-flow.

Acknowledgement: Thanks are due to Dr Petri Peltonen (Geological Survey of Finland) for arranging the mineral separation procedure, to Dr Anton Antonov (VSEGEI, St Petersburg, Russia) for providing some BSE and CL images, and to many colleagues for helpful discussions. We thank the Royal Society for financial support in the form of a Joint International Reseach Project.

References

[1] Rudnick R.L., Williams I.S., Dating the lower crust by ion microprobe. Earth Planet. Sci. Lett., 1987, 85, 145–161.

[2] Downes H., Peltonen P., Manttari L., Sharkov E.V., Proterozoic zircon ages from lower crustal granulite xenoliths, Kola Peninsula, Russia: evidence for crustal growth and reworking. J. Geol. Soc., 2002, 159, 485–488.

[3] Peltonen P., Manttari I., Huhma H., Whitehouse M.J., Multi-stage origin of the lower crust of the Karelian craton from 3.5 to 1.7 Ga based on isotopic ages of kimberlite- derived mafic granulite xenoliths. Precambrain Res., 2006 147, 107–123.
[4] Koreshkova M.Yu., Downes H., Nikitina L.P., Vladykin N.V., Larionov A.N., Sergeev S.A., Trace element and age characteristics of zircons in granulite xenoliths from the Udachnaya kimberlite pipe, Siberia. Precambrain Res., 2009, 168, 197–212.
[5] Rossi P., Cocherie A., Fanning C.M., Deloule E., Variscan to eo-Alpine events recorded in European lower-crust zircons sampled from the French Massif Central and Corsica, France. Lithos, 2006, 87, 235–260.
[6] Horvath F., Bada G., Szafian P., Tari G., Adam A., Cloetingh S., Formation and deformation of the Pannonian Basin: constraints from observational data. In: Geological Society of London Memoir 32, European Lithosphere Dynamics, Gee D.G., Stephenson R.A. (Eds.), 2006, 191–206.
[7] Csontos L., Vörös A., Mesozoic plate tectonic reconstructions of the Carpathian region. Palaeogeogr. Palaeoclimatol. Palaeoecol., 2004, 210, 1–56.
[8] Tari G., Dunkl I., Horvath F., Lenkey L., Szafian P., Toth T., Vakarcs, G., Lithospheric structure of the Pannonian basin derived from seismic, gravity and geothermal data. In: Durand B., Jolivet L., Horvat, F., Seranne M. (Eds.): The Mediterranean basins: Tertiary extension within the Alpine Orogen. Geol. Soc. London Spec. Publ., 1999, 156, 215–250.
[9] Fodor L., Csontos L., Bada G., Benkovics L., Gyorfi I., Tertiary tectonic evolution of the Pannonian basin system and neighbouring orogens: a new synthesis of palaeostress data. In: Durand B., Jolivet L., Horvath F., Seranne M. (Eds.): The Mediterranean basins: Tertiary extension within the Alpine Orogen. Geol. Soc. London Spec. Publ., 1999, 156, 295–334.
[10] Szafian P., Horvath F., Crustal structure in the Carpatho-Pannonian region: insights from three-dimensional gravity modelling and their geodynamic significance. Int. J Earth Sci., 2005, 95, 50–67.
[11] Horvath F., Towards a quantitative model for the Pannonian Basin. Tectonophysics, 1993, 226, 333–358.
[12] Lenkey L., Dövenyi P., Horvath F., Cloetingh S.A.P.L., Geothermics of the Pannonian basin and its bearing on the neotectonics. EGU Stephan Mueller Special Publication Series, 2002, 3, 29–40.
[13] Bodri L., Geothermal model of the Earth's crust in the Pannonian Basin. Tectonophysics, 1981, 79, 225–236.
[14] Embey-Isztin A., Scharbert H.G., Deitrich H., Poultidis H., Petrology and geochemistry of peridotite xenoliths in alkali basalts from the Transdanubian Volcanic Region, West Hungary. J. Petrol., 1989, 30, 79–105.
[15] Embey-Isztin A., Scharbert H.G., Deitrich H., Poultidis H., Mafic granulite and clinopyroxenite xenoliths from the Transdanubian Volcanic Region (Hungary): implications for the deep structure of the Pannonian Basin. Mineral. Mag., 1990, 54, 463–483.
[16] Embey-Isztin A., Downes H., Kempton P.D., Dobosi G., Thirlwall M.F., Lower crustal granulite xenoliths from the Pannonian Basin, Hungary. Part 1: mineral chemistry, thermobarometry and petrology. Contrib. Mineral. Petr., 2003, 144, 652–670.
[17] Wijbrans J., Nemeth K., Martin U., Balogh K., $^{40}Ar/^{39}Ar$ geochronology of Neogene phreatomagmatic volcanism in the western Pannonian Basin, Hungary. J Volcanol. Geoth. Res., 2007, 164, 193–204.
[18] Kempton P.D., Downes H., Embey-Isztin, A., Mafic granulite xenoliths in Neogene alkali basalts from the western Pannonian Basin: insights into the lower crust of a collapsed orogen. J. Petrol., 1997, 38, 941–970.
[19] Dobosi G., Kempton P.D., Downes H., Embey-Isztin A., Thirlwall M.F., Greenwood P., Lower crustal granulite xenoliths from the Pannonian Basin, Hungary. Part 2: Sr-Nd-Pb-Hf and O isotope evidence for formation of continental lower crust by tectonic emplacement of oceanic crust. Contrib. Mineral. Petr., 2003, 144, 671–683.
[20] Török K., Dégi J., Szep A., Marosi Gy., Reduced carbonic fluids in mafic granulite xenoliths from the Bakony-Balaton Highland volcanic field, W-Hungary. Chem. Geol., 2005, 223, 93–108.
[21] Dégi J., Abart R., Török K., Rhede D., Petrishcheva E. . Evidence for xenolith- host basalt interaction from chemical patterns in Fe-Ti oxides from mafic granulite xenoliths from the Bakony-Balaton volcanic field (W-Hungary). Miner. Petrol., 2009, 95, 219–234.
[22] Dégi J., Abart R., Török K., Bali E., Wirth R., Rhede D., Symplectite formation during decompression induced garnet breakdown in lower crustal mafic granulite xenoliths: mechanisms and rates. Contrib. Mineral. Petr., 2010, 159, 293–314.
[23] Kovács I., Szabó C., Petrology and geochemistry of granulite xenoliths beneath the Nógrád-Gömör volcanic field, Carpathian-Pannonian region (N-Hungary/S-Slovakia). Miner. Petrol., 2005, 85, 269–290.
[24] Csontos L., Nagymarosy A., Horvath F., Kovac M., Tertiary evolution of the intra-Carpathian area: A model. Tectonophysics, 1992, 208, 221–241.
[25] Lelkes-Felvari G., Sassi F.P., Outlines of the pre-Alpine metamorphisms in Hungary. In: Karamara S., Sassi F.P. (Eds.) IGCP No 5. Newsletter, 1981, 3, 193–195.
[26] Svojtka M., Koš J., Venera Z., Dating granulite-facies structures and the exhumation of lower crust in the Moldanubian Zone of the Bohemian Massif. Int. J. Earth Sci., 2001, 91, 373–385.
[27] Pearce N.J.G., Perkins W.T., Westgate J.A., Gorton M.P., Jackson S.E., Neal C.R., Chenery S.P.. A compilation of new and published major and trace element data for NIST SRM 610 and NIST SRM 612 glass reference materials. Geostand. Geoanal. Res., 1997, 21, 115–144.
[28] Cumming G.L., Richards J.R., Ore lead isotope ratios in a continuously changing Earth. Earth Planet. Sci. Lett., 1975, 28, 155–171.
[29] Ludwig K., Isoplot 3.0. Berkeley Geochronology Center Special Publication, 2003, 4.
[30] Williams I.S. U-Th-Pb geochronology by ion microprobe. Reviews in Economic Geology, 1998, 7, 1–35.
[31] Ludwig K.R., SQUID 1.03, A User's Manual; Berkeley Geochronology Center Special Publication, 2001, 2, 19.
[32] Black L.P. et al., Improved $^{206}Pb/^{238}U$ microprobe geochronology by monitoring of a trace-element-related matrix effect; SHRIMP, ID-TIMS, ELA-ICP-MS and oxygen isotope documentation for a seriesof zircon standards. Chem. Geol., 2004, 205, 115–140.
[33] Claoué-Long J.C., Compston W., Roberts J., Fanning C.M., Two Carboniferous ages: a comparison of SHRIMP zircon dating with conventional zircon ages and 40Ar/39Ar analysis. In: Geochronology, Time Scales and Global Stratigraphic Correlation, Berggen W.A., Kent D.V., Aubry M.P., Hardenbol J. (Eds.), SEPM Special Publication, 1995, 4, 3–21.

[34] Steiger R.H, Jäger E., Subcommission on geochronology: convention on the use of decay constants in geochronology and cosmochronology. Earth Planet. Sci. Lett., 1977, 36, 359–362.

[35] Stacey J.S., Kramers J. D., Approximation of terrestrial lead isotope evolution by a two-stage model. Earth Planet. Sci. Lett., 1975, 26, 207–221.

[36] Corfu F., Hanchar J.M., Hoskin P.W.O., Kinny P., Atlas of zircon textures. In: Hanchar J.M., Hoskin P.W.O. (Eds.), Zircon, Rev. Mineral. Geochem., 2003, 53, 469–495.

[37] Alvarez-Valero A.M., Kreigsman L.M., Crustal thinning and mafic underplating beneath the Neogene Volcanic Province (Betic Cordillera, SE Spain): evidence from crustal xenoliths. Terra Nova, 2007, 19, 266–271.

[38] Wilde S.A., Zhou X., Nemchin A.A., Sun, M., Mesozoic crust-mantle interaction beneath the North China Craton: a consequence of the dispersal of Gondwanaland and accretion of Asia. Geology, 2003, 31, 817–820.

[39] Fernandez-Suares J., Arenas R., Jeffries T.E., Whitehouse M.J., Villaseca C.. A U-Pb study of zircons from a lower crustal granulite xenolith of the Spanish Central System: a record of Iberian lithospheric evolution from the Neoproterozoic to the Triassic. J. Geol., 2006, 114, 471–483.

[40] Roberts M.P., Finger F., Do U-Pb zircon ages from granulites reflect peak metamorphic conditions? Geology, 1997, 25, 319–322.